
Universiteit
Leiden
The Netherlands

The diverse roles of integrin α3β1 in cancer: Lessons learned from skin and breast carcinogenesis

Ramovš, V.

Citation
Ramovš, V. (2021, February 18). *The diverse roles of integrin α3β1 in cancer: Lessons learned from skin and breast carcinogenesis*. Retrieved from https://hdl.handle.net/1887/3135050

Version:	Publisher's Version
License:	Licence agreement concerning inclusion of doctoral thesis in the Institutional Repository of the University of Leiden
Downloaded from:	https://hdl.handle.net/1887/3135050

Note: To cite this publication please use the final published version (if applicable).

Cover Page

Universiteit Leiden

Leiden University Repository

The handle http://hdl.handle.net/1887/3135050 holds various files of this Leiden University dissertation.

Author: Ramovš, V.
Title: The diverse roles of integrin α3β1 in cancer: Lessons learned from skin and breast carcinogenesis
Issue date: 2021-02-18

INTEGRIN α3β1 IS A KEY REGULATOR OF SEVERAL PRO-TUMORIGENIC PATHWAYS DURING SKIN CARCINOGENESIS

Published in Journal of Investigative Dermatology (2020)
(online ahead of print, doi: 0.1016/j.jid.2020.07.024)

Veronika Ramovs, Ana Krotenberg Garcia[#], Maaike Kreft, Arnoud Sonnenberg

Division of Cell Biology, The Netherlands Cancer Institute, Amsterdam, the Netherlands
#Current address: Division of Molecular Pathology, The Netherlands Cancer Institute, Amsterdam

Correspondence to Arnoud Sonnenberg: a.sonnenberg@nki.nl

ABSTRACT

Integrin α3β1 plays a crucial role in tumor formation in the two-stage chemical carcinogenesis model (DMBA/TPA treatment). However, the mechanisms whereby the expression of α3β1 influences key oncogenic drivers of this established model are not known yet. Using an in vivo mouse model with epidermal deletion of α3β1 and in vitro Matrigel cultures of transformed keratinocytes, we demonstrate the central role of α3β1 in promoting activation of several pro-tumorigenic signaling pathways during the initiation of DMBA/TPA-driven tumorigenesis. In transformed keratinocytes, α3β1-mediated FAK/Src-activation leads to in vitro growth of spheroids and to strong Akt and Stat3 activation, when the α3β1-binding partner tetraspanin CD151 is present to stabilize cell-cell adhesion and to promote Smad2 phosphorylation. Remarkably, α3β1 and CD151 can support Akt and Stat3 activity independently of α3β1 ligation by laminin-332 and as such control essential survival signals required for suprabasal keratin-10 expression during keratinocyte differentiation. These data demonstrate that α3β1 together with CD151 regulate signaling pathways that control the survival of differentiating keratinocytes and provide mechanistic understanding of the essential role of α3β1 in early stages of skin cancer development.

INTRODUCTION

Over the last few decades, the two-stage chemical carcinogenesis mouse model (DMBA/TPA treatment) has enabled a better understanding of key players and complex processes occurring during different stages of cutaneous cancer. This established model consists of a single application of carcinogen DMBA, causing an activating mutation in Hras1 gene, followed by bi-weekly applications of the phorbol ester TPA, stimulating an increased production of growth factors and inflammatory cytokines. This leads to sustained epidermal hyperplasia and development of benign tumors papillomas, which can progress to invasive carcinomas upon further TPA treatment [1]. The most prominent factors leading to papilloma development are stromal and inflammatory responses, and activation of several growth factor signaling pathways [2,3]. In addition to the Raf/MEK/ERK cascade [4,5], resulting from the activating *Hras1* mutation and TPA treatment, FAK/Src [6–8], PI3K/Akt [9,10], JAK/Stat3 [11–13] and TGFβ/Smad [14,15] signaling pathways play a central role in tumor development.

We previously showed that integrin α3β1 is also required for the development of papillomas upon DMBA/TPA treatment [16]. Yet, how α3β1 affects known key drivers of this model has not been elucidated. Integrins constitute a family of transmembrane glycoproteins that mediate cell-matrix adhesion, but also function as bidirectional transducers of mechano- and biochemical signals. They play diverse roles in tumorigenesis and tumor progression [17]. Integrin α3β1 often exerts opposing functions in cancer, switching from a tumor promoting to suppressing mechanism, depending on the cancer type/driving mechanism, cell environment and stage of the disease [18, 19]. Together with integrin α6β4, α3β1 mediates cell-matrix adhesion of basal keratinocytes by binding the extracellular matrix (ECM) proteins laminin-332 and -511. Furthermore, α3β1 can stabilize E-cadherin-based cell-cell junctions, especially when forming a complex with the tetraspanin CD151 [18]. Here, we investigate the impact of α3β1 on activation of several key signaling pathways during the initiation phase of mouse skin tumorigenesis. Our study uncovers the crucial role of α3β1 in activation of FAK, Akt and Stat3 in transformed keratinocytes and thus provides mechanistic understanding of the tumor-promoting function of α3β1 during skin carcinogenesis.

RESULTS AND DISCUSSION

Integrin α3β1 is required for efficient activation of Stat3, Akt and FAK signaling during the initiation phase of DMBA/TPA tumorigenesis *in vivo*

In order to assess the impact of α3β1 on DMBA/TPA-mediated pro-tumorigenic signaling, we subjected mice with an epidermis-specific deletion of α3β1 (*Itgα3*-KO mice) and wild-type mice (*Itgα3*-WT mice) to topical short-term DMBA/TPA treatment, when pro-tumorigenic pathways are switched on, but tumors have not yet been formed (**Fig. 1a**).

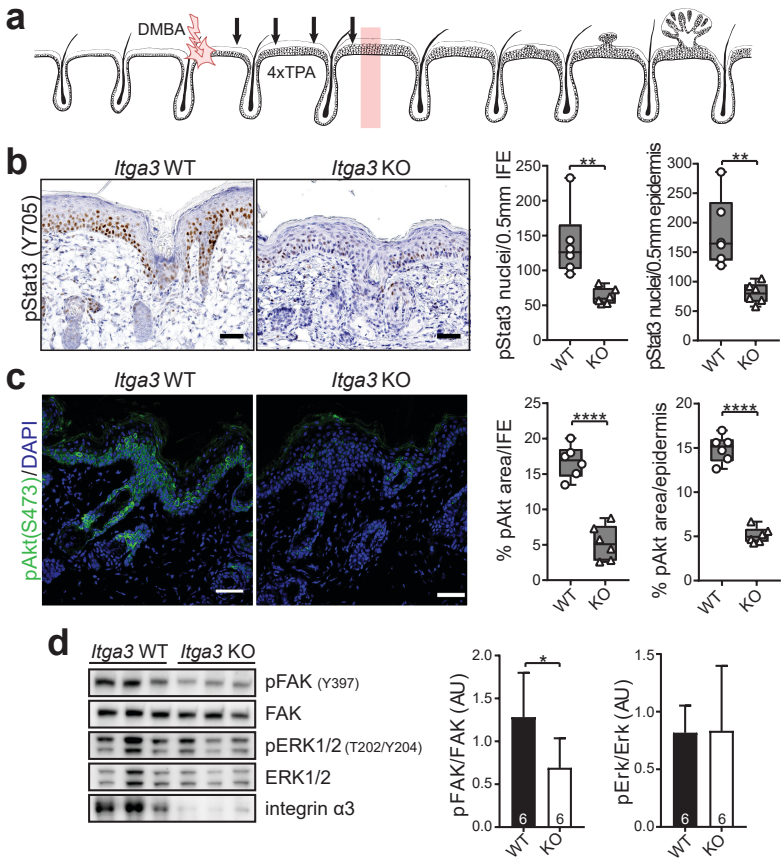

Figure 1: Integrin α3β1 is required for full activation of Stat3, Akt and FAK signaling during the initiation of DMBA/TPA tumorigenesis *in vivo*. (**a**) Overview of the short-term DMBA/TPA treatment (Box: time of analysis). (**b-d**) Analysis of the epidermis, isolated from short-term DMBA/TPA-treated *Itgα3*-WT and -KO mice. (**b**) Representative IHC images and quantification of the number of pStat3 (Y705)-positive nuclei in the 500 µm of interfollicular or total epidermis. Box and whisker plot, dot = mouse (average of 8 quantified images). (**c**) IF images of pAkt staining and quantifications of pAkt-positive area in interfollicular or total epidermis. Box and whisker plot, dot = mouse (average of 10 quantified images). (**d**) WB and quantifications of the protein levels of pFAK Y397 and pERK1/2 (T202/Y204) of 6 *Itgα3*-WT and -KO mice (mean±SD). IFE, interfollicular epidermis. Scale: 50 µm. Statistics: unpaired t test, *P<0.05, **P<0.005, ****P<0.0001.

Signaling through the IL-6/JAK/STAT3 and PI3K/Akt/mTOR pathways are critical for the initiation and progression of papillomas [9–12,20]. Epidermal depletion of α3β1 compromises both pathways, as judged by the strong reduction of the activity of Stat3 and Akt in the epidermis of *Itgα3*-KO compared to -WT mice (**Fig. 1b-c**). We also observed a reduction of phosphorylated FAK (pFAK) in short-term DMBA/TPA treated skin of *Itgα3*-KO mice (**Fig. 1d**). However, the loss of α3β1 did not affect pERK1/2 (**Fig. 1d**), which is consistent with unperturbed phosphorylation of ERK1/2 in *Stat3*-KO mice [12]. The reduction of active FAK upon the deletion of α3β1 is in line with the role of integrin-mediated adhesion in FAK/Src signaling [17], and the requirement of FAK for development of papillomas in mice [7].

Together, this data demonstrates that α3β1 is required for full activation of the Stat3, Akt and FAK pro-tumorigenic signaling pathways during the first stage of skin tumorigenesis.

α3β1-mediated activation of Stat3, Akt and FAK/Src is crucial for 3D growth of transformed keratinocytes *in vitro*

To further investigate the role of α3β1 in pro-tumorigenic signaling, we made use of *Hras1* transformed keratinocytes, isolated from *Itgα3*-WT mice that underwent full DMBA/TPA treatment (MSCC *Itgα3*-KO and -WT keratinocytes) [16]. Consistent with the lack of tumorigenesis in two-stage carcinogenesis [16] and the reduced pro-tumorigenic signaling in *Itgα3*-KO mice, the growth of MSCC keratinocytes in 3D Matrigel depended on the presence of α3β1 and its ability to support Stat3 and Akt signaling (**Fig. 2a-c**). The ability of α3β1 to support growth of transformed keratinocytes is in line with the high-level expression of α3β1 (**Supplementary fig. 1a**) and the activity of Stat3 [12] and Akt [21] in papillomas, as well as with Akt- and Stat3-dependent progression of the cell cycle via activation of cyclin D during DMBA/TPA-treatment [9,12]. Interestingly, MSCC spheroids exhibited co-dependent activation of Stat3 and Akt: while treatment with Akt (MK2206) or mTOR (AZD8055) inhibitors ablated Stat3 activity (**Fig. 2a**), treatment with Stat3 inhibitors (niclosamide, stattic) strongly reduced phosphorylation of Akt (**Fig. 2b, Supplementary fig. 1b**). In line with this, the expression of constitutively activated Stat3 (CA-Stat3) in *Itgα3*-KO keratinocytes restored Akt activation and vice versa, the expression of myristoylated Akt (myrAkt), which renders Akt constitutively active, activated Stat3 (**Fig. 2a-b**). Such crosstalk between the PI3K/Akt and Stat3 pathways has been demonstrated before in different types of tumors [22–24]. Furthermore, several functional links have been established between Stat3 and Akt signaling pathways, such as TEC kinases, which activate Stat3 downstream of PI3K [25] and phosphoinositide-dependent kinase 1, which is a master regulator of Akt and has been shown to be a direct transcriptional target of Stat3 in melanomas [26].

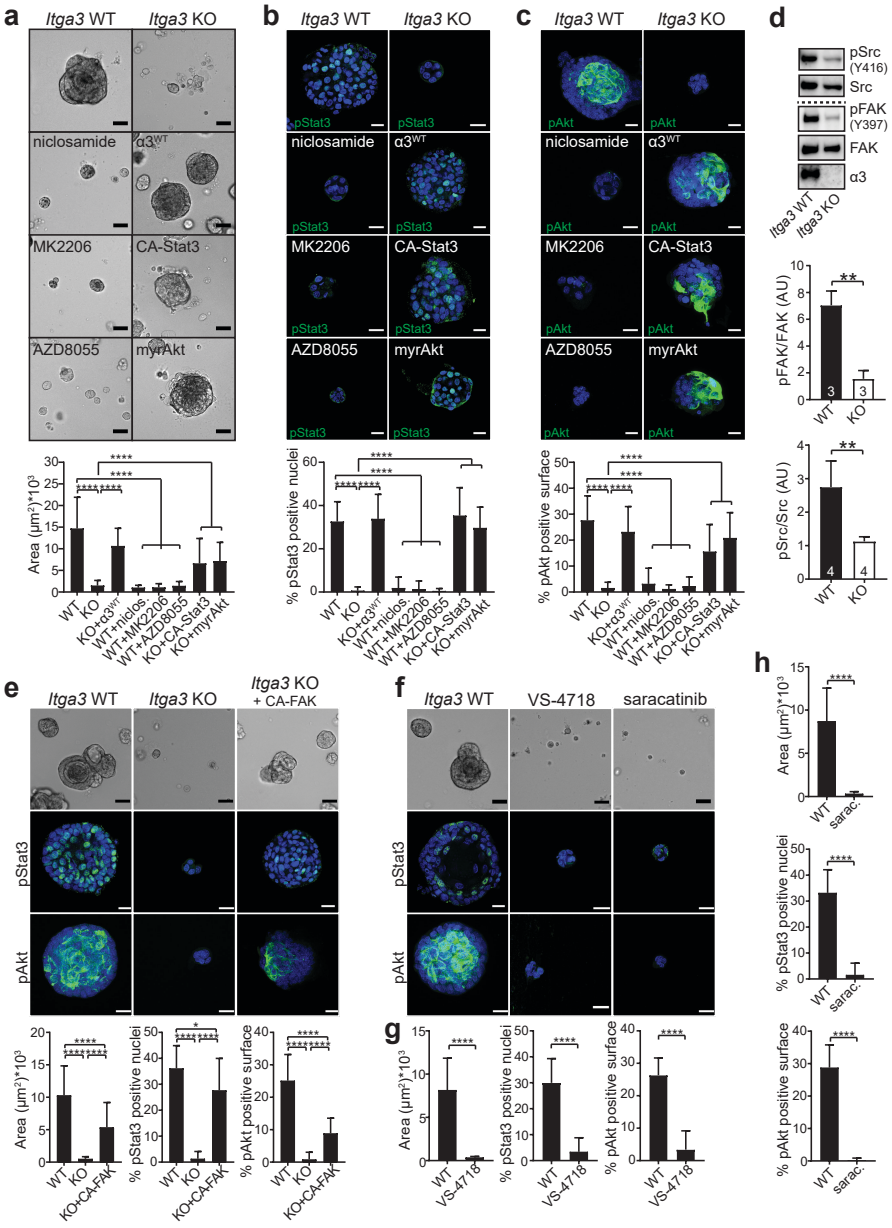

Figure 2: α3β1-mediated activation of Stat3, Akt and FAK/Src is crucial for 3D growth of transformed keratinocytes *in vitro*. (**a-c**) Analysis of *Itga3*-WT spheroids, treated with 2µM niclosamide, 10µM MK2206, or 500nM AZD8055 and *Itga3*-KO spheroids, transfected with wild-type α3 (α3^{WT}), constitutively active Stat3 (CA-Stat3), or myristoylated Akt (MyrAkt). (**a**) Bright-field images and quantifications (n=80-95) of the spheroid area. (**b**) IF images of z-slice and quantifications (n=29-30) of pStat3 (Y705)-positive nuclei. (**c**) IF images of maximum intensity projection and quantifications (n=30) of pAkt (S473)-positive area. (**d**) WB and quantification show reduced pFAK (Y397) and pSrc

(Y416) protein levels in *Itgα3*-KO compared to WT spheroids. (**e**) Representative bright field/IF images and quantifications of the area (n=80), pStat3 (Y705)-positive nuclei (n=20) and pAkt (S473)-positive area (n=20) of *Itgα3*-KO, WT, and *Itgα3*-KO spheroids transfected with constitutively active FAK (CA-FAK) construct. (**f-h**) Representative bright field/IF images and quantifications of the area (n=80), pStat3 (Y705)-positive nuclei (n=21-26) and pAkt (S473)-positive area (n=20-26) of non-treated, 10μM saracatinib-treated and 5μM VS-4718-treated *Itgα3*-WT spheroids. Scale: 20μm (IF), 50μm (bright field). Statistics: mean ± SD, d, f, h: unpaired t test, a-c, e: Sidak's multiple comparisons test, *P<0.05, **P<0.005, ****P<0.0001.

Consistent with our *in vivo* data (**Fig. 1d**), the absence of α3β1 in spheroids resulted in reduced activation of FAK, as well as Src (**Fig. 2d**). The FAK/Src complex presents a likely link between α3β1 and the PI3K/Akt and Stat3 pathways [27–29]. This hypothesis is supported by our finding that *Itgα3*-KO spheroids expressing constitutively active FAK (CA-FAK) (**Supplementary Fig. 1b**) showed an increased Stat3 activation and, albeit moderately, increased Akt activation and 3D growth (**Fig. 2e**). Likewise, FAK and Src inhibition by VS-4718 and saracatinib (AZD0530), respectively, ablated the activation of Akt and Stat3, and inhibited 3D growth of transformed keratinocytes (**Fig. 2f-h**).

Our results strongly suggest that α3β1 promotes growth of papillomas via FAK/Src signaling, which supports co-dependent activation of the PI3K/Akt and Stat3 signaling pathways.

Integrin α3β1 can support Stat3 and Akt signaling independently of its ligation by laminin

In hyperplastic DMBA/TPA-treated skin, pStat3 and pAkt-positive keratinocytes can be observed in both basal and suprabasal cell layers of the epidermis (**Fig. 1b-c, 3a**). In fact, suprabasal keratinocytes often exhibit elevated levels of pAkt compared to basal cells (**Fig. 3a**), which is consistent with previous observations [30]. Such high suprabasal activity of Akt and Stat3 is surprising considering the fact that laminin-332 and -511, the ligands of α3β1, are only found in the basement membrane, underlying the basal keratinocytes (**Fig. 3b**). Because in hyperplastic mouse skin, α3β1 is also expressed by suprabasal, differentiating keratinocytes (**Fig. 3b**), unconventionally, α3β1 may support pro-tumorigenic Stat3 and Akt signaling independently of its ligation by laminin. To test this hypothesis, we reconstituted *Itgα3*-KO MSCC keratinocytes with either wild-type human α3 ($\alpha3^{WT}$) or an α3 mutant ($\alpha3^{G163A}$), which is unable to bind to laminin-332 [31] (**Supplementary fig 2a-b**). The MSCC-$\alpha3^{WT}$ and -$\alpha3^{G163A}$ keratinocytes grown in spheroids exhibit tight cell-cell adhesion with laminin-332 deposited only by cells forming the outermost basal cell layer (**Fig. 3c**). In these cells, α3β1 localizes at the cell-ECM interface. Additionally, α3β1 is present in the inner cell layers at cell-cell contacts (**Fig. 3c**). Consistent with our *in vivo* observations, ligation of α3β1 to laminin-332 was not needed for strong activation of Stat3 and Akt (**Fig. 3d-e**). The

expression of α3^{G163A} also almost completely restored growth of spheroids (**Fig. 3d-e**). This was further confirmed by inhibiting α3β1 ligation to laminin-332 using function-blocking J143 antibody, which did not have any effect on Akt or Stat3 activation or on 3D keratinocyte growth (**Supplementary fig. 2c**). Integrin signaling has been conventionally linked to ligation of integrins by ECM proteins, leading to their association with actomyosin cytoskeleton and activation of FAK and Src family kinases [32]. Even though the expression of α3^{G163A} leads to reduced FAK activation and a small decrease in Src phosphorylation (**Fig. 3f**), Itga3-KO spheroids exhibit a much more prominent reduction of FAK/Src signaling (**Fig. 2d**). Thus, α3β1 can support FAK/Src activation at the level, sufficient to drive Stat3 and Akt signaling, independently of its ligation by laminin-332. Non-ligated α3β1 may mediate phosphorylation of FAK directly if clustered by other integrins or integrin-associated proteins. Alternatively, α3β1 may support the activation of other integrins, which promote FAK phosphorylation.

We conclude that α3β1 is present in cell-cell contacts also in suprabasal keratinocytes, where it supports Akt and Stat3 signaling independently of its ligation by laminin-332.

Deletion of CD151 impairs cell-cell contact integrity, resulting in reduced activation of Stat3 and Akt but not reduced FAK/Src signaling

The role of integrins in cell-cell contacts is poorly understood. Integrin α3β1 is known to stabilize cell-cell contacts [33] and to associate with E-cadherin [34]. The ability of α3β1 to control cell-cell junction stability is dependent on its binding to tetraspanin CD151 [35–38], a tumor-promoter in DMBA/TPA carcinogenesis model [39,40]. Furthermore, CD151 has been shown to promote TPA-induced Stat3 phosphorylation in mouse and human keratinocytes [39]. We thus wondered whether α3β1-CD151 complexes play a central role in pro-tumorigenic signaling, especially in suprabasal cells. Interestingly, we observed reduced expression of CD151 in the epidermis of *Itga3*-KO compared to -WT mice (**Fig. 4a, Supplementary fig. 3a-b**), which is in line with observations in leukemic K562 cells [41-42]. Since it was shown that suppression of α3β1 expression by RNAi affects clustering of CD151 and promotes its homodimerization [43-44], our data may suggest that the stability of CD151 in mouse epidermis depends on its ability to form a complex with α3β1. As expected, deletion of CD151 in MSCC keratinocytes using CRISPR/Cas9 technology with two distinct guide RNAs (*Cd151*-KO G1 and G2) destabilized cell-cell contacts in spheroids, as observed by staining for E-cadherin and the presence of a laminin-332 matrix between keratinocytes in the inner cell layers of the spheroids (**Fig. 4b**). Furthermore, *CD151*-KO MSCCs exhibited decreased Smad2 phosphorylation, which is induced by TGFβ and promoted by association of α3β1 and E-cadherin [34] (**Fig. 4c**). We observed reduced pSmad2 also in the epidermis of *Itga3*-KO mice (**Fig. 4d, Supplementary fig. 3c**), demonstrating a role of α3β1-CD151 in

sustaining the pro-tumorigenic TGFβ/Smad2/3 pathway [14,15]. The deletion of *Cd151* in MSCCs resulted in strongly reduced pAkt and in impaired nuclear translocation of pStat3 (**Fig. 4e**). Remarkably, the reduced activity of Akt and Stat3 did not affect the 3D growth of *Cd151*-KO keratinocytes (**Fig. 4e**). A similar trend was observed when spheroids were grown in the presence of the E-cadherin function-blocking antibody DECMA-1 (**Supplementary fig. 3d**), further supporting a role of CD151 and cell-cell junctions in promoting Stat3 and Akt activity.

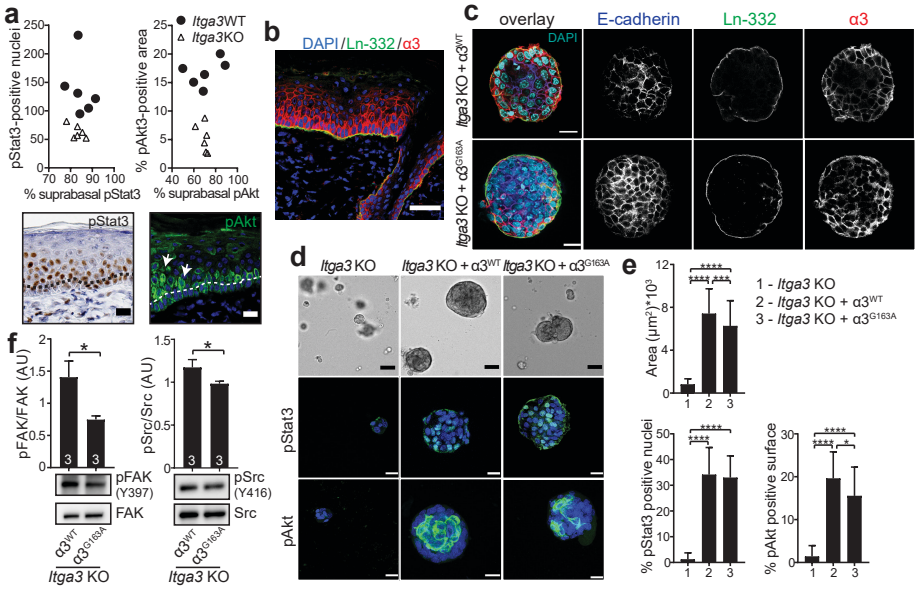

Figure 3: α3β1 supports Stat3 and Akt signaling independently of its ligation by laminin matrix. (**a**) Quantifications (dot=mouse, averaged 8 images) and representative images of the percentage of pStat3-positive nuclei and pAkt-positive area located suprabasally in the short-term DMBA/TPA-treated interfollicular epidermis of *Itga3*-KO and WT mice. Dotted line delineates suprabasal keratinocytes. High pAkt expression is commonly observed in suprabasal keratinocytes (arrows). (**b**) IF image of short-term DMBA/TPA-treated *Itga3*-WT epidermis. α3β1 colocalizes with laminin-332 in the basement membrane but is also expressed in cell-cell contacts suprabasally (Scale: 50 μm). (**c**) IF images of *Itga3*-KO spheroids, transfected with wild-type α3 ($α3^{WT}$) or laminin-binding mutant G163A ($α3^{G163A}$). α3β1 co-localizes with laminin-332 at the outer layer of spheroids and with E-cadherin in cell-cell contacts (scale: 20μm). (**d-e**) Representative bright field/IF images and quantifications of the area (n=80-115), pStat3 (Y705)-positive nuclei (n=30) and pAkt (S473)-positive area (n=26-30) of *Itga3*-KO spheroids and *Itga3*-KO spheroids expressing either $α3^{WT}$ or $α3^{G163A}$ (Scale: 20 μm (IF), 50 μm (bright field)). (**f**) WB and quantification showing levels of pFAK (Y397) and pSrc (Y416) in MSCC-$α3^{WT}$ and -$α3^{G163A}$ spheroids. Statistics: mean ± SD, e: Sidak's multiple comparisons test, f: unpaired t test, *P<0.05, ***P<0.0005, ****P<0.0001.

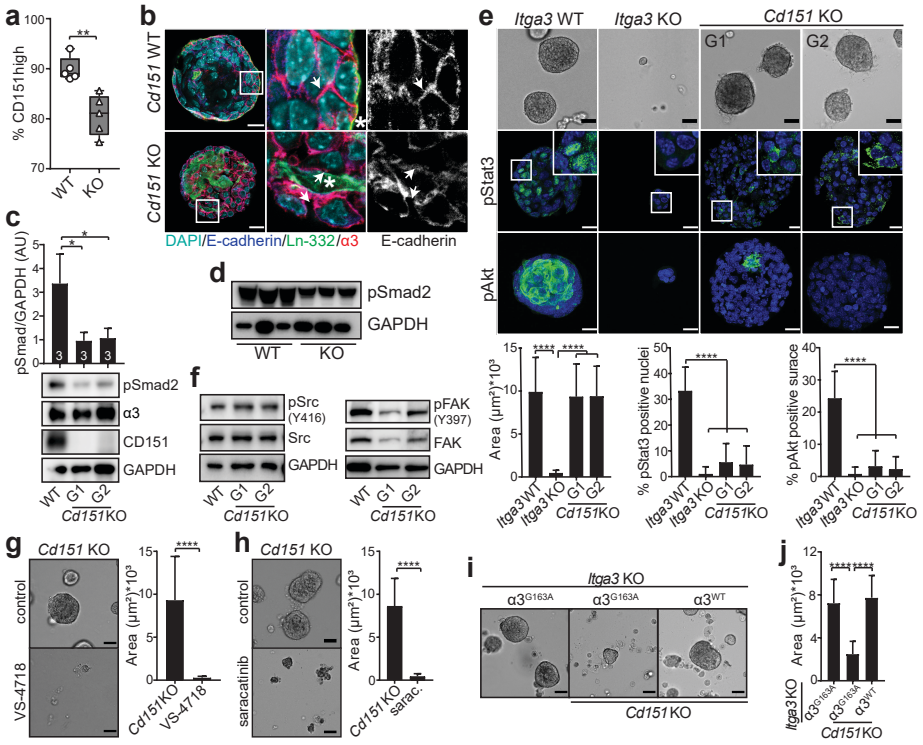

Figure 4: Deletion of CD151 reduces cell-cell contact integrity, resulting in reduced activation of Stat3 and Akt but not reduced FAK/Src signaling. (**a**) Flow cytometry quantification showing reduced expression of CD151 upon the deletion of α3β1 in epidermis. Box and whisker plot, dot = mouse (gating strategy: Figure S3a). (**b**) IF staining for laminin-332, α3β1, and E-cadherin of WT and *Cd151*-KO spheroids shows reduced cell-cell contacts (arrow) and localization of laminin-332 in inner keratinocyte layers (asterisk) in the absence of CD151 (Scale: 20µm). (**c**) WB with quantifications showing reduced pSmad2 (S465/467) in Cd151-KO spheroids. (**d**) WB showing reduced pSmad2 (S465/467) in the epidermis of short-term DMBA/TPA-treated Itga3-KO, compared to WT mice (quantification: Figure S3c). (**e**) Representative bright field/IF images and quantifications of the area (n=80), pStat3 (Y705)-positive nuclei (n=22-25) and pAkt (S473)-positive area (n=28) of of *Itga3*-KO and WT spheroids and *Itga3*-WT spheroids with deletion of *Cd151*, obtained with two distinct CRISPR/Cas9 gRNAs (G1 and G2) (Scale: 20 µm (IF), 50 µm (bright field)). (**f**) WB showing comparable levels of pSrc (Y416) and pFAK (Y397) in WT and *Cd151*-KO spheroids (quantification: Figure S3e). (**g-h**) Representative bright-field images and quantifications (n=80) of the size of *Cd151*-KO spheroids treated with (g) 10 µM saracatinib and (**h**) 5 µM VS-4718 (Scale: 50µm). (**i**) Bright-field images and (j) quantifications (n=85) of the size of MSCC-α3^{G163A} spheroids and MSCC-α3^{WT} and α3^{G163A} spheroids with deletion of *Cd151* (Scale: 50 µm). Statistics: mean ± SD, a, g-h: unpaired t test, c, e, j: Sidak's multiple comparisons test, *P<0.05, **P<0.005, ****P<0.0001.

Because *Cd151*-KO and -WT spheroids showed similar levels of active Src and FAK (**Fig. 4f, Supplementary fig. 3d**), we wondered whether 3D growth of these spheroids depends primarily on FAK/Src signaling. Inhibition of FAK and Src impaired the growth of Cd151-KO spheroids (**Fig. 4g-h**), thus demonstrating that FAK/Src signaling supports

proliferation of these cells, despite their low Akt and Stat3 activity. Since α3β1-mediated adhesion to laminin-332 increases FAK activation (**Fig. 3f**), the presence of laminin-332 and α3β1 in the inner layers of Cd151-KO spheroids (**Fig. 4b**) could promote ECM-adhesion-supported pro-survival signaling and thus explain their sole dependency on FAK/Src signaling for growth. Indeed, the deletion of CD151 in MSCC-α3^{G163A} cells and treatment of and MSCC-α3^{WT} *Cd151*-KO spheroids with function-blocking J143 antibody resulted in strongly reduced spheroid size (**Fig. 4i-j, Supplementary fig. 3f-g**). However, it should be noted that the levels of pFAK and pSrc were comparable in MSCC-α3^{G163A} and MSCC-α3^{G163A} *Cd151*-KO spheroids (**Fig. S3h**) but higher than those observed in *Itga3*-KO spheroids (**Fig. 2d**, **3f**). Therefore, α3β1 can still support some FAK/Src activity independently of laminin or CD151-association.

Together, our data shows that even though FAK/Src activation is required, it is not sufficient to support Akt and Stat3 signaling in our model. In transformed keratinocytes, efficient Akt and Stat3 activation also depends on the cell-cell contact-stabilizing function of CD151, a binding partner of α3β1.

α3β1 and CD151 are needed for 3D growth of differentiating keratinocytes

Previous studies showed that Akt and Stat3 play important roles in the differentiation of keratinocytes [9,45]. While Stat3 signaling prevents terminal differentiation of keratinocytes through regulation of the transcription factor AP-1 [45], activation of Akt promotes the survival of differentiating keratinocytes [30,46]. The activation of PI3K/Akt in primary mouse keratinocytes occurs concomitantly with the expression of keratinocyte differentiation markers and, as in *Itga3*-WT MSCC spheroids, depends on the E-cadherin-mediated adhesion and the activity of the Src family kinases [30]. We therefore wondered whether α3β1 and CD151 play a role in the differentiation of MSCCs through the regulation of Akt and Stat3 signaling. In *Itga3*-WT MSCC spheroids we could observe a single outer layer of keratin-14 positive basal keratinocytes that adhere to laminin-332 and express integrin α6β4, and a variable number of inner, post-mitotic suprabasal cells that express keratin-10 (**Fig. 5a and Supplementary fig. 4a**). The *Itga3*-KO spheroids were small, containing only a few α6β4-expressing keratinocytes and no keratin-10-positive cells. Interestingly, several of the keratinocytes in the outer cell layer of MSCC-α3^{G163A} spheroids exhibited expression of keratin-10 together with laminin-332. As this was not found in WT spheroids, it is likely that α3β1-laminin-332 ligation prevents aberrant differentiation (**Fig. 5a**). Strikingly, none of the *CD151*-KO keratinocytes expressed keratin-10, while laminin-332 colocalized with α6β4 in addition to α3β1 in outer and inner layers of the spheroids (**Fig. 4a and 5a**). Furthermore, consistent with the roles of Akt and Stat3 in promoting survival of differentiating

keratinocytes, activated Akt and Stat3 could be observed in the keratin-10-positive differentiating *Itgα3*-WT and $\alpha3^{G163A}$ transformed keratinocytes (**Fig. 5b**).

Thus, while sustained 3D growth of basal-like *Cd151*-KO keratinocytes primarily depends on FAK/Src signaling and less on strong activity of Akt and Stat3, the growth of spheroids that similarly to papillomas contain differentiating keratinocyte layers requires FAK/Src, Stat3 and Akt activation (**Fig. 2a,b and g**).

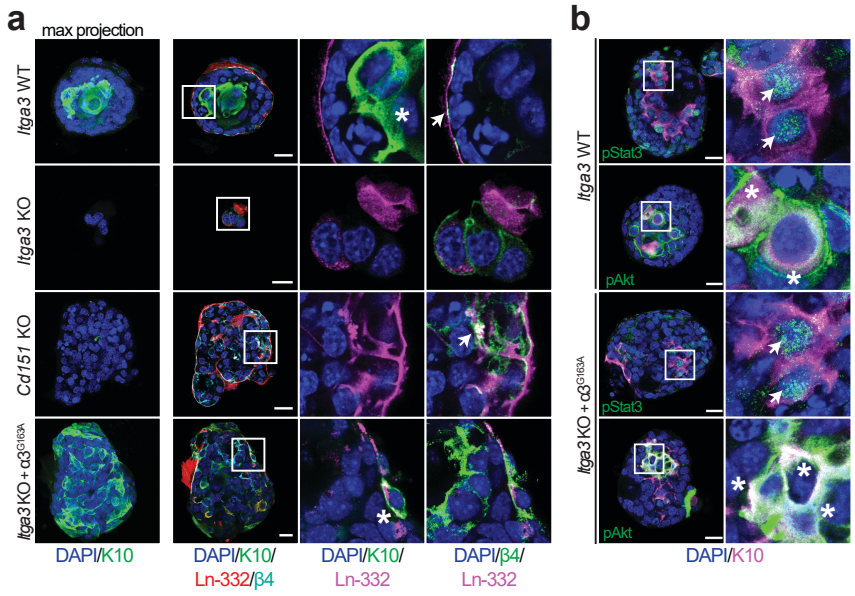

Figure 5: α3β1 and CD151 are needed for 3D growth of differentiating keratinocytes. (**a**) IF staining shows the absence of differentiation marker keratin-10 (asterisk) and co-localization of integrin α6β4 and laminin-332 (arrow) in the inner layers of spheroids in the absence of Cd151. Such basal-like phenotype is largely absent in *Itgα3*-KO spheroids, transfected with laminin-binding mutant G163A ($\alpha3^{G163A}$), which show high expression of keratin-10 and its localization with laminin-332 in outer spheroid layers (asterisk). (**b**) IF staining shows the presence of pAkt (asterisk) and nuclear localization of pStat3 (arrows) in keratin-10-positive *Itgα3*-WT and *Itgα3*-KO spheroids expressing $\alpha3^{G163A}$. Scale: 20 μm

Final remarks

We previously showed that *Itgα3*-KO and *Cd151*-KO mice displayed increased epidermal turnover and loss of slow-cycling stem cells [16,40,47]. However, skin thickness and number of proliferative keratinocytes were similar between *Itgα3*-KO and WT mice during DMBA/TPA treatment (**Supplementary fig. 4b**) [16], which suggests that the increased rate of proliferation is coupled with enhanced differentiation to maintain the faster turnover of keratinocytes in the *Itgα3*-KO mice. The question, therefore, arises how to relate these observations to our present findings. In *Itgα3*-KO mice, decreased Stat3

and Akt activity may accelerate terminal differentiation of the suprabasal keratinocytes, leading to increased rate of proliferation of basal keratinocytes and the loss of slow-cycling cells. As it is generally accepted that DMBA-initiated basal keratinocytes must persist long enough in hyperplastic skin to acquire additional mutations leading to outgrowth of clonal papillomas, eventual tumor outgrowth could depend on the Akt and Stat3-regulated survival of suprabasal keratinocytes. However, the increased epidermal turnover can be detected also in non-treated skin of Itga3-KO mice, where α3β1 is mostly restricted to the basal keratinocytes in much thinner epidermis. Thus, the loss of stem cells is DMBA/TPA-primed skin of *Itga3*-KO mice is likely caused by a combination of a reduced adhesion strength of *Itga3*-KO basal keratinocytes, reflected in reduced FAK/Src activation, and an increased rate of terminal differentiation, promoted by decreased Akt and Stat3 activation in α3β1-depleted suprabasal keratinocytes.

In conclusion, α3β1 is a key regulator of several pro-tumorigenic pathways during initiation of DMBA/TPA-mediated tumorigenesis. In transformed keratinocytes, α3β1-mediated FAK/Src-activation leads to strong Akt and Stat3 signaling when CD151 is present, promoting cell-cell stability and Smad2 phosphorylation. Remarkably, α3β1-CD151 can support Akt and Stat3 activity independently of α3β1 ligation by laminin-332 and as such promote pro-survival signaling in suprabasal differentiating keratinocytes, which likely delays epidermal turnover and enables eventual papilloma formation. For tumor outgrowth transformed keratinocytes depend on CD151-independent α3β1-mediated FAK/Src activation, which promotes proliferation of basal keratinocytes, and on α3β1-CD151 mediated Stat3 and Akt activation in suprabasal layers, which is required for 3D growth of differentiating transformed keratinocytes (**Fig. 6**).

MATERIALS AND METHODS

Animal experiments

Epidermis-specific Krt14$^{tm1(cre)Wbm}$; *Itga3*$^{tm1Son/tm1Son}$ (*Itga3*-KO mice) and Krt14$^{tm1(cre)Wbm}$ (*Itga3*-WT mice) on FVB/N background have been previously described [16]. DMBA/TPA tumorigenesis has been done as before [16]. Briefly, backs of 6-week old mice were shaved and after a week topically treated with 30μg (in 200μl acetone) of DMBA (Sigma, D3254), followed by bi-weekly topical applications of 12,34μg (in 200μl acetone) of TPA (Sigma, P1585) for 20 weeks. For short-term DMBA/TPA treatment mice were treated with four doses of TPA over two weeks following DMBA treatment. Thereafter, mice were killed, skin was isolated and processed for immunofluorescence, immunohistochemistry analysis and/or protein lysate preparation. All animal studies were performed according to Dutch guidelines for care and use of laboratory animals and were approved by the animal welfare committee of the Netherlands Cancer Institute.

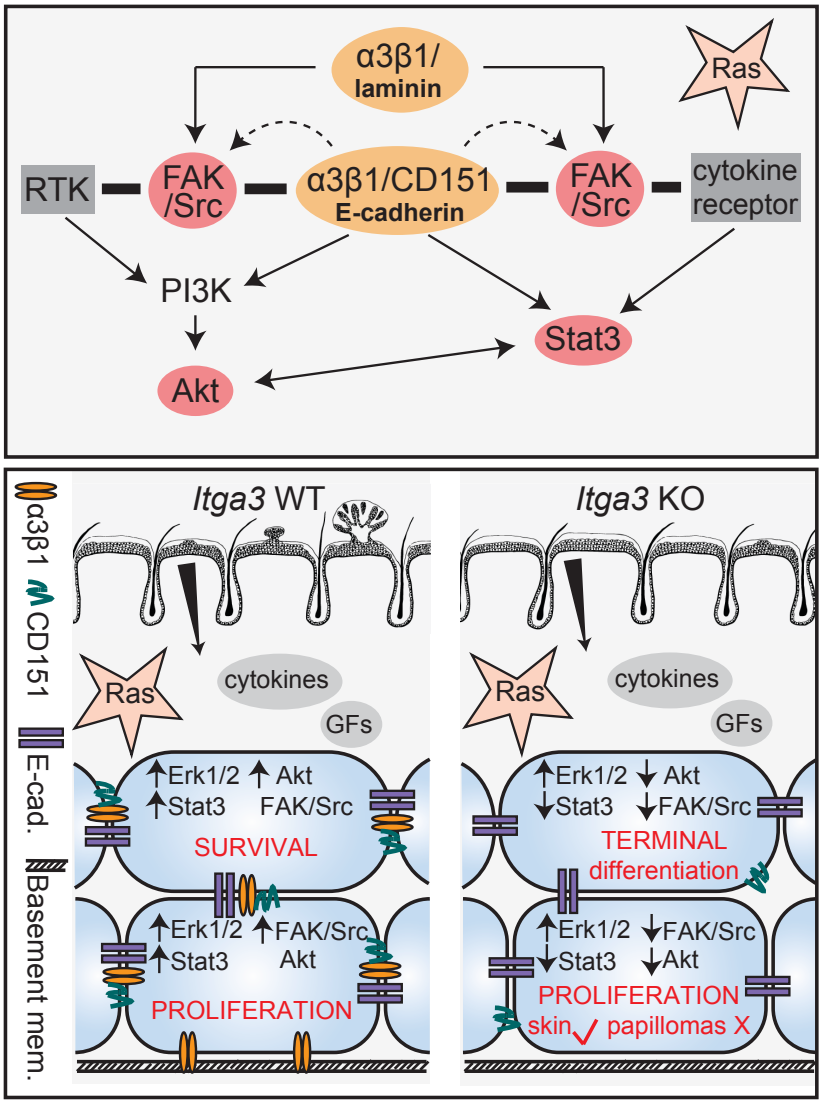

Figure 6: The model of α3β1-mediated pro-tumorigenic signaling in transformed keratinocytes. In *Hras1*-transformed keratinocytes, integrin-mediated FAK/Src-activation leads to strong Akt and Stat3 activation when CD151 is present, promoting cell-cell adhesion stability (top). Basal keratinocytes in hyperplastic skin during the initiation of tumorigenesis proliferate regardless of the presence of α3β1, which supports moderate induction of pAkt and strong activation of Stat3 and FAK/Src in this layer. In suprabasal keratinocytes, α3β1 is not ligated by laminin-332 but localizes to cell-cell contacts with its binding partner CD151. Here, CD151 and α3β1 induce pro-survival Stat3 and Akt signaling, which delays terminal differentiation of suprabasal keratinocytes. This allows outgrowth of well-differentiated papillomas, which need α3β1-mediated FAK/Src activation in basal keratinocytes for proliferation and Stat3 and Akt activation in basal/suprabasal layers for eventual outgrowth (bottom). RTK: receptor tyrosine kinase; GF: growth factor.

Cell culture and generation of stable cell lines

To obtain *Itgα3*-KO MSCC cells, stably expressing wild-type α3 (MSCC *Itgα3*-KO $\alpha3^{WT}$), full-length human α3A cDNA was ligated into pUC18-a3. After digestion with SphI, α3A cDNA was ligated into LZRS-IRES-zeo, a modified LZRS retroviral vector conferring resistance to zeocin [48]. Retroviral vector was introduced into the Phoenix packaging cells by the calcium phosphate precipitation method, and virus-containing supernatant was collected [48]. MSCC *Itgα3*-KO cells were infected with the recombinant virus by the 1,2-dioleoyl-3-trimethylammonio-propane (DOTAP) method (Boehringer). After infection overnight at 37°C, infected cells were selected with 0.2 mg ml^{-1} zeocin (Invitrogen). Cells expressing α3β1 were obtained by fluorescence activated cell sorting. To obtain *Itgα3*-KO MSCC cells, stably expressing laminin-binding mutant $\alpha3^{G163A}$ [31] (MSCC-$\alpha3^{G163A}$), $\alpha3^{G163A}$ in pBJ-1 expression vector (a kind gift of Yoshikazu Takada, University of California, Davis, USA) was transfected using Lipofectamine 2000 (Invitrogen) following the manufacturer's instructions and bulk populations were sorted for α3-expressing cells using fluorescence activated cell sorting. Retroviral expression vector pBABE-puro with construct encoding constitutively active Stat3 [49] (a kind gift of D. Peeper, NKI, the Netherlands) or active myristoylated Akt [50] (a kind gift of R. Bernards, NKI, the Netherlands) was used to generate MSCC *Itgα3*-KO CAStat3 and MSCC *Itgα3*-KO myrAkt cells, using retroviral transduction as described above. Cells expressing CAStat3 or myrAkt were selected with 5μg/ml of puromycin (Invitrogen). MSCC *Itgα3* KO cells expressing constitutively active FAK (MSCC *Itgα3*-KO CAFAK) were obtained by lentiviral transduction of the pLV-neo-CD2-FAK vector (#37013 Addgene; deposited by Bob Weinberg [51]) followed by 600 μg ml^{-1} of G-418 solution (Roche).

To generate CD151-deficient MSCC keratinocytes, target sgRNAs against *Cd151* (Guide1: 5'-GTTCCGTCGCTCCTTGAAAGTGG -3' and Guide2: 5'- CACGGCCTACATCTTAGTGGTGG-3') were cloned into pX330-U6-Chimeric_BB-CBh-hSpCas9 (#42230 Addgene; deposited by Feng Zhang [52]). Cells were transfected with plasmids containing sgRNA using Lipofectamine 2000 (Invitrogen) following the manufacturer's instructions. CD151-negative cell lines were obtained by fluorescent activated cell sorting. MSCC-$\alpha3^{WT}$ *Cd151*-KO and MSCC-$\alpha3^{G163A}$ *Cd151*-KO keratinocytes were generated as described above using sgRNA guide 1.

All cell lines were cultured in DMEM with 10% heat-inactivated FCS and antibiotics at 37°C in a humidified, 5% CO_2 atmosphere.

Matrigel cell culture

For 3D cell culture, 70μl of growth factor-reduced Matrigel Basement Membrane Matrix (Corning, 354230) was pipetted per well of 96-well plate and incubated for 30min at

37°C. 1000 cells in cold DMEM containing 10%FCS and 2% Matrigel were seeded on top of the Matrigel layer and grown for 7 days with or without inhibitors/function-blocking antibodies.

For the size measurements, spheroids were imaged with Zeiss AxioObserver Z1 inverted microscope, utilizing 5x and 10x objectives and a Hamamatsu ORCA AG Black and White CCD camera and using Zeiss ZEN software. Area of the spheroids was measured manually using ImageJ [53,54].

For inhibition studies, MSCC cells were seeded with 10 μM saracatinib, 10 μM MK2206, 500 nM AZD8055, 5 μM VS-4718 or 2 μM niclosamide (Selleckchem) or 2 μM stattic (Selleckchem) added to the DMEM with 10% heat-inactivated FCS and antibiotics. For function-blocking experiments, MSCC were grown in Matrigel in the presence of 10 μg ml^{-1} of anti-α3 J143 [55] or anti E-cadherin DECMA-1 antibody (Life technologies, 16-3249-82). Spheroids were retrieved from Matrigel by incubation with Cell recovery solution (Corning, 354253) for 1h at 4°C and subsequent resuspension in ice-cold PBS. For BrdU treatment, spheroids were incubated for 4h before harvesting with 50μM of BrdU (DakoCytomation).

Antibodies

For IHC, primary antibodies were used: rabbit- anti pStat3 Y705 (Cell Signaling, #9145, 1:100), rabbit anti-Ki67 (Abcam, ab15580, 1:3000) and mouse anti-integrin α3 (Santa Cruz, sc-374242, 1:500). For IF, we used primary antibodies: goat anti-mouse integrin α3 (R&D, AF2787, 1:50), mouse anti-human integrin α3 J143 ([49], 1:100), rabbit anti-pStat3 Y705 (Cell Signaling, 9131S, 1:100), rabbit anti-pAkt S473 (Cell Signaling, 9271, 1:100), rat anti-integrin β4 (BD Pharm., 346.11A, 1:50), rabbit anti-laminin-332 R14 (1:400, kind gift of M. Aumailey), rabbit anti-keratin 14 (Covance, PRB-155P, 1:400), rat anti-E-cadherin DECMA-1 (Life technologies, 16-3249-82, 1:100), mouse anti-BrdU (DakoCytomation, 1:50), mouse anti-E-cadherin (BD bioscience, #610182, 1:100) and mouse anti-keratin 10 DE-K10 (non-diluted supernatant, kind gift of D. Ivanyi [56]). For secondary antibodies we used 1:200 of goat-anti rabbit Alexa Fluor 488, donkey anti-rabbit Alexa Fluor 594, donkey anti-goat Alexa Fluor 488, donkey anti-goat Alexa Fluor 647, donkey anti-rat Alexa Fluor 488, goat anti-rat Alexa Fluor 647, donkey anti-mouse Alexa Fluor 647 and goat anti-mouse Alexa Fluor 568 (Invitrogen). For flow cytometry we used primary rat anti-CD151 (R&D, MAB4609, 1:50) and mouse anti-human integrin α3 J143 ([55], 1:100) antibodies. For secondary antibodies donkey anti-rat PE (Biolegend, #406421; 1:200 dilution) and donkey anti-mouse PE (Biolegend, #406421; 1:200 dilution) were used. For western blot, we used primary antibodies: rabbit anti-pFAK Y397 (Invitrogen, 44-624G, 1:1000), mouse anti-FAK (BD transduction lab., #610087, 1:1000), rabbit anti-pERK1/2

T202/Y204 (Cell Signaling, #4376s, 1:1000), rabbit anti-ERK1/2 (Cell signaling, #9102, 1:1000), rabbit anti-integrin α3 (homemade, 1:2000), rabbit anti-pSrc Y416 (Cell signaling, #2101, 1:1000), rabbit anti-Src (Cell signaling, #2123, 1:1000), rabbit anti-CD151 140190 ([57], 1:500), rabbit anti-pSmad2 S465/467 (Cell signaling, #3108S, 1:1000), mouse anti-GAPDH (Calbiochem, CB1001, 1:1000) and mouse anti-tubulin (Sigma, B-5-1-2, 1:5000). As secondary antibodies we used stabilized goat anti-mouse HRP-conjugated and stabilized goat anti-rabbit HRP-conjugated (BioRad).

Immunohistochemistry

Tumors and skin were isolated, fixed in EAF and/or formaldehyde, embedded in paraffin, sectioned and stained. Images were taken with the Aperio ScanScope (Aperio, Vista, CA, USA), using ImageScope software version 12.0.0 (Aperio). Count of phospho-Stat3 positive nuclei was performed blindly. Image analysis was performed using ImageJ [53,54].

Immunofluorescence

Skin was isolated, embedded in Tissue-Tek OCT (optimal cutting temperature) cryoprotectant and frozen. Frozen skin was cryosectioned, sections were fixed in ice-cold acetone and blocked with 2% bovine serum albumin (BSA, Sigma) in PBS for 1h at room temperature. Isolated spheroids were mounted on Poly-L-Lysine (Santa Cruz, 25988-63-0)-coated slides, fixed in 4% paraformaldehyde in PBS for 10 min, permeabilized with 0.2% Triton-X-100 for 5 min, and blocked with PBS containing 2% BSA for 1h at room temperature. Tissues or spheroids were incubated with primary antibodies in 2% BSA in PBS overnight, followed by incubation with secondary antibodies diluted 1:200 for 60-90 min. All samples where counterstained with DAPI for 5 min at room temperature. Cryosections were mounted in Vectashield (Vector Laboratories H-1000) and skin sections in mowiol. Samples were analyzed by Leica TCS SP5 confocal microscope with 40 and 63x (NA 1.4) oil objectives. When spheroids were analyzed, the thickness of spheroids was determined and z-stacks with step size every 1.2-1.3µm were acquired. All images were processed using ImageJ [53,54]. The number of pStat3 positive nuclei was manually counted in total mouse epidermis, interfollicular mouse epidermis and in three separate images per z-stack. In spheroids the percentage of pStat3-positive nuclei was calculated by dividing the number of pStat3-positive nuclei in image with total number of nuceli based on DAPI staining. Percentage of pAkt-positive area in mouse epidermis was calculated using the Analyze Particle function, with delineated total or interfollicular epidermis as a region of interest (ROI). Percentage of pAkt-positive area in spheroids was calculated on maximum intensity projected z-stacks, with delineated surface of spheroids based on DAPI staining as a ROI. pAkt-positive area was divided by the total ROI area to define the percentage of pAkt-positive area.

Flow cytometry

Keratinocytes were isolated from mouse back skin as described before [58] or MSSC keratinocytes were trypsinized. Cells were further washed in PBS containing 2% FCS, incubated for 1h at 4°C with primary antibody in PBS 2% FCS, washed and incubated with secondary antibody for 30 min at 4°C. Cells were analyzed on a Becton Dickinson FACS Calibur analyzer after addition of the indicated life/dead cell marker. For fluorescence activated cell sorting, α3-positive or CD151-negative cell populations were obtained using a Becton Dickinson FACSAria IIu cell sorter.

Western Blotting

Protein lysates were obtained from keratinocytes, isolated from mouse back skin as described before [52], from isolated spheroids, or from sub-confluent cell cultures by lysis in RIPA buffer (20 mM Tris-HCl (pH 7.5), 100 mM NaCl, 4 mM EDTA (pH 7.5), 1% Nonidet P-40, 0.1% SDS, 0.5% sodium deoxycholate) supplemented with 1.5 mM Na_3VO_4, 15 mM NaF (Cell Signaling) and protease inhibitor cocktail (Sigma). Lysates were cleared by centrifugation at 14.000 x g for 20 min at 4°C and eluted in sample buffer (50 mM Tris-HCl pH 6.8, 2% SDS, 10% glycerol, 12.5 mM EDTA, 0.02% bromophenol blue) with final concentration of 2% β-mercaptoethanol and denatured at 95°C for 10 min. Proteins were separated by electrophoresis using Bolt Novex 4–12% gradient Bis-Tris gels (Invitrogen), transferred to Immobilon-P transfer membranes (Millipore Corp) and blocked for 1h in 2% BSA in TBST buffer (10 mM Tris (pH 7.5), 150 mM NaCl, and 0.3% Tween-20). The blocked membranes were incubated overnight at 4°C with primary antibodies in TBST containing 2% BSA. After washing, membranes were incubated for 1 h with horseradish peroxidase–conjugated goat anti-mouse IgG or goat anti-rabbit IgG (diluted 1:5000 in 2% BSA in TBST buffer). After washing, the bound antibodies were detected by enhanced chemiluminescence using or Clarity™ Western ECL Substrate (Bio-Rad) or Amersham ECL Western Blotting Detection Reagent (GE Healthcare) as described by the manufacturer. Signal intensities were quantified using ImageJ [53,54].

Adhesion assay

For adhesion assays, 6-well plates were coated with laminin-332-rich matrix, obtained by growing RAC-11P cells [59] to complete confluence, after which the plates were washed

with PBS and incubated with 20 mM EDTA in PBS overnight at 4°C. The RAC-11P cells were then removed by pipetting and washing with PBS, $1*10^5$ MSCC cells were seeded on the laminin-332-rich matrix and left to grow overnight. Images of cells, showing different ability to spread on laminin-matrix, were obtained with a Zeiss AxioObserver

Z1 inverted microscope, utilizing 5x and 10x objectives, a Hamamatsu ORCA AG Black and White CCD camera, and Zeiss ZEN software.

Statistical Analysis

Statistical analysis was performed using GraphPad Prism (version 7.0c). Unpaired two-tailed t test was used for comparisons of experimental groups with a control group. Experiments with more than two experimental groups were analyzed using one-way ANOVA. Planned comparisons were conducted using Sidak's multiple comparison test after a global ANOVA was determined to be significant. Results with P-value lower than 0.05 were considered significantly different from the null hypothesis.

ACKNOWLEDGMENTS

We would like to thank Yoshikazu Takada, Daniel Peeper and Rene Bernards for sharing their reagents. We would also like to acknowledge Alba Zuidema, Coert Margadant and Roy Zent for useful discussions and for proofreading of the manuscript.

REFERENCES

[1] E.L. Abel, J.M. Angel, K. Kiguchi, J. DiGiovanni, Multi-stage chemical carcinogenesis in mouse skin: Fundamentals and applications, Nat Protoc. 4 (2009) 1350–1362. https://doi.org/10.1038/nprot.2009.120.

[2] P.Y. Huang, A. Balmain, Modeling cutaneous squamous carcinoma development in the mouse, Cold Spring Harb Perspect Med. 4 (2014) a013623. https://doi.org/10.1101/cshperspect.a013623.

[3] J.E. Rundhaug, S.M. Fischer, Molecular Mechanisms of Mouse Skin Tumor Promotion, Cancers (Basel). 2 (2010) 436–482. https://doi.org/10.3390/cancers2020436.

[4] C. Bourcier, A. Jacquel, J. Hess, I. Peyrottes, P. Angel, P. Hofman, P. Auberger, J. Pouysségur, G. Pagès, p44 Mitogen-Activated Protein Kinase (Extracellular Signal-Regulated Kinase 1)–Dependent Signaling Contributes to Epithelial Skin Carcinogenesis, Cancer Res. 66 (2006) 2700–2707. https://doi.org/10.1158/0008-5472.CAN-05-3129.

[5] F.A. Scholl, P.A. Dumesic, D.I. Barragan, K. Harada, J. Charron, P.A. Khavari, Selective role for Mek1 but not Mek2 in the induction of epidermal neoplasia, Cancer Res. 69 (2009) 3772–3778. https://doi.org/10.1158/0008-5472.CAN-08-1963.

[6] T. Matsumoto, J. Jiang, K. Kiguchi, L. Ruffino, S. Carbajal, L. Beltrán, D.K. Bol, M.P. Rosenberg, J. DiGiovanni, Targeted expression of c-Src in epidermal basal cells leads to enhanced skin tumor promotion, malignant progression, and metastasis, Cancer Res. 63 (2003) 4819–4828.

[7] G.W. McLean, N.H. Komiyama, B. Serrels, H. Asano, L. Reynolds, F. Conti, K. Hodivala-Dilke, D. Metzger, P. Chambon, S.G.N. Grant, M.C. Frame, Specific deletion of focal adhesion kinase suppresses tumor formation and blocks malignant progression, Genes Dev. 18 (2004) 2998–3003. https://doi.org/10.1101/gad.316304.

[8] B. Serrels, A. Serrels, S.M. Mason, C. Baldeschi, G.H. Ashton, M. Canel, L.J. Mackintosh, B. Doyle, T.P. Green, M.C. Frame, O.J. Sansom, V.G. Brunton, A novel Src kinase inhibitor reduces tumour formation in a skin carcinogenesis model, Carcinogenesis. 30 (2009) 249–257. https://doi.org/10.1093/carcin/bgn278.

[9] C. Segrelles, J. Lu, B. Hammann, M. Santos, M. Moral, J.L. Cascallana, M.F. Lara, O. Rho, S. Carbajal, J. Traag, L. Beltrán, A.B. Martínez-Cruz, R. García-Escudero, C. Lorz, S. Ruiz, A. Bravo, J.M. Paramio, J. DiGiovanni, Deregulated activity of Akt in epithelial basal cells induces spontaneous tumors and heightened sensitivity to skin carcinogenesis, Cancer Res. 67 (2007) 10879–10888. https://doi.org/10.1158/0008-5472.CAN-07-2564.

[10] A. Suzuki, S. Itami, M. Ohishi, K. Hamada, T. Inoue, N. Komazawa, H. Senoo, T. Sasaki, J. Takeda, M. Manabe, T.W. Mak, T. Nakano, Keratinocyte-specific Pten deficiency results in epidermal hyperplasia, accelerated hair follicle morphogenesis and tumor formation, Cancer Res. 63 (2003) 674–681.

[11] B. Ancrile, K.-H. Lim, C.M. Counter, Oncogenic Ras-induced secretion of IL6 is required for tumorigenesis, Genes Dev. 21 (2007) 1714–1719. https://doi.org/10.1101/gad.1549407.

[12] K.S. Chan, S. Sano, K. Kiguchi, J. Anders, N. Komazawa, J. Takeda, J. DiGiovanni, Disruption of Stat3 reveals a critical role in both the initiation and the promotion stages of epithelial carcinogenesis, J. Clin. Invest. 114 (2004) 720–728. https://doi.org/10.1172/JCI21032.

[13] D.J. Kim, K. Kataoka, D. Rao, K. Kiguchi, G. Cotsarelis, J. Digiovanni, Targeted disruption of stat3 reveals a major role for follicular stem cells in skin tumor initiation, Cancer Res. 69 (2009) 7587–7594. https://doi.org/10.1158/0008-5472.CAN-09-1180.

[14] R. Pérez-Lorenzo, L.M. Markell, K.A. Hogan, S.H. Yuspa, A.B. Glick, Transforming growth factor beta1 enhances tumor promotion in mouse skin carcinogenesis, Carcinogenesis. 31 (2010) 1116–1123. https://doi.org/10.1093/carcin/bgq041.

[15] A.G. Li, S.-L. Lu, M.-X. Zhang, C. Deng, X.-J. Wang, Smad3 Knockout Mice Exhibit a Resistance to Skin Chemical Carcinogenesis, Cancer Res. 64 (2004) 7836–7845. https://doi.org/10.1158/0008-5472.CAN-04-1331.

[16] N. Sachs, P. Secades, L. van Hulst, M. Kreft, J.-Y. Song, A. Sonnenberg, Loss of integrin α3 prevents skin tumor formation by promoting epidermal turnover and depletion of slow-cycling cells, Proc Natl Acad Sci U S A. 109 (2012) 21468–21473. https://doi.org/10.1073/pnas.1204614110.

[17] H. Hamidi, J. Ivaska, Every step of the way: integrins in cancer progression and metastasis, Nature Reviews Cancer. 18 (2018) 533. https://doi.org/10.1038/s41568-018-0038-z.

[18] C.S. Stipp, Laminin-binding integrins and their tetraspanin partners as potential antimetastatic targets, Expert Rev Mol Med. 12 (2010). https://doi.org/10.1017/S1462399409001355.

[19] Ramovs V, Te Molder L, Sonnenberg A. The opposing roles of laminin-binding integrins in cancer. Matrix Biol J Int Soc Matrix Biol. 2016 Aug 22;

[20] T.D. Carr, R.P. Feehan, M.N. Hall, M.A. Rüegg, L.M. Shantz, Conditional disruption of rictor demonstrates a direct requirement for mTORC2 in skin tumor development and continued growth of established tumors, Carcinogenesis. 36 (2015) 487–497. https://doi.org/10.1093/carcin/bgv012.

[21] C. Segrelles, S. Ruiz, P. Perez, C. Murga, M. Santos, I.V. Budunova, J. Martínez, F. Larcher, T.J. Slaga, J.S. Gutkind, J.L. Jorcano, J.M. Paramio, Functional roles of Akt signaling in mouse skin tumorigenesis, Oncogene. 21 (2002) 53–64. https://doi.org/10.1038/sj.onc.1205032.

[22] S.-S. Han, H. Yun, D.-J. Son, V.S. Tompkins, L. Peng, S.-T. Chung, J.-S. Kim, E.-S. Park, S. Janz, NF-κB/STAT3/PI3K signaling crosstalk in iMycEμ B lymphoma, Mol Cancer. 9 (2010) 97. https://doi.org/10.1186/1476-4598-9-97.

[23] E. Kim, M. Kim, D.-H. Woo, Y. Shin, J. Shin, N. Chang, Y.T. Oh, H. Kim, J. Rheey, I. Nakano, C. Lee, K.M. Joo, J.N. Rich, D.-H. Nam, J. Lee, Phosphorylation of EZH2 activates STAT3 signaling via STAT3 methylation and promotes tumorigenicity of glioblastoma stem-like cells, Cancer Cell. 23 (2013) 839–852. https://doi.org/10.1016/j.ccr.2013.04.008.

[24] J.M. Blando, S. Carbajal, E. Abel, L. Beltran, C. Conti, S. Fischer, J. DiGiovanni, Cooperation between Stat3 and Akt signaling leads to prostate tumor development in transgenic mice, Neoplasia. 13 (2011) 254–265. https://doi.org/10.1593/neo.101388.

[25] P.K. Vogt, J.R. Hart, PI3K and STAT3: a new alliance, Cancer Discov. 1 (2011) 481–486. https://doi.org/10.1158/2159-8290.CD-11-0218.

[26] M.E. Picco, M.V. Castro, M.J. Quezada, G. Barbero, M.B. Villanueva, N.B. Fernández, H. Kim, P. Lopez-Bergami, STAT3 enhances the constitutive activity of AGC kinases in melanoma by transactivating PDK1, Cell Biosci. 9 (2019) 3. https://doi.org/10.1186/s13578-018-0265-8.

[27] N.P. Visavadiya, M.P. Keasey, V. Razskazovskiy, K. Banerjee, C. Jia, C. Lovins, G.L. Wright, T. Hagg, Integrin-FAK signaling rapidly and potently promotes mitochondrial function through STAT3, Cell Commun. Signal. 14 (2016) 32. https://doi.org/10.1186/s12964-016-0157-7.

[28] Y. Pylayeva, K.M. Gillen, W. Gerald, H.E. Beggs, L.F. Reichardt, F.G. Giancotti, Ras- and PI3K-dependent breast tumorigenesis in mice and humans requires focal adhesion kinase signaling, J. Clin. Invest. 119 (2009) 252–266. https://doi.org/10.1172/JCI37160.

[29] H. Xia, R.S. Nho, J. Kahm, J. Kleidon, C.A. Henke, Focal Adhesion Kinase Is Upstream of Phosphatidylinositol 3-Kinase/Akt in Regulating Fibroblast Survival in Response to Contraction of Type I Collagen Matrices via a β1 Integrin Viability Signaling Pathway, J. Biol. Chem. 279 (2004) 33024–33034. https://doi.org/10.1074/jbc.M313265200.

[30] E. Calautti, J. Li, S. Saoncella, J.L. Brissette, P.F. Goetinck, Phosphoinositide 3-kinase signaling to Akt promotes keratinocyte differentiation versus death, J. Biol. Chem. 280 (2005) 32856–32865. https://doi.org/10.1074/jbc.M506119200.

[31] X.P. Zhang, W. Puzon-McLaughlin, A. Irie, N. Kovach, N.L. Prokopishyn, S. Laferté, K. Takeuchi, T. Tsuji, Y. Takada, Alpha 3 beta 1 adhesion to laminin-5 and invasin: critical and differential role of integrin residues clustered at the boundary between alpha 3 N-terminal repeats 2 and 3, Biochemistry. 38 (1999) 14424–14431.

[32] Z. Sun, S.S. Guo, R. Fässler, Integrin-mediated mechanotransduction, J. Cell Biol. 215 (2016) 445–456. https://doi.org/10.1083/jcb.201609037.

[33] F. Zhang, C.C. Tom, M.C. Kugler, T.-T. Ching, J.A. Kreidberg, Y. Wei, H.A. Chapman, Distinct ligand binding sites in integrin alpha3beta1 regulate matrix adhesion and cell-cell contact, J. Cell Biol. 163 (2003) 177–188. https://doi.org/10.1083/jcb.200304065.

[34] Y. Kim, M.C. Kugler, Y. Wei, K.K. Kim, X. Li, A.N. Brumwell, H.A. Chapman, Integrin alpha3beta1-dependent beta-catenin phosphorylation links epithelial Smad signaling to cell contacts, J. Cell Biol. 184 (2009) 309–322. https://doi.org/10.1083/jcb.200806067.

[35] N. Chattopadhyay, Z. Wang, L.K. Ashman, S.M. Brady-Kalnay, J.A. Kreidberg, α3β1 integrin–CD151, a component of the cadherin–catenin complex, regulates PTPμ expression and cell–cell adhesion, J Cell Biol. 163 (2003) 1351–1362. https://doi.org/10.1083/jcb.200306067.

[36] J.L. Johnson, N. Winterwood, K.A. DeMali, C.S. Stipp, Tetraspanin CD151 regulates RhoA activation and the dynamic stability of carcinoma cell-cell contacts, J. Cell. Sci. 122 (2009) 2263–2273. https://doi.org/10.1242/jcs.045997.

[37] S.C. Zevian, J.L. Johnson, N.E. Winterwood, K.S. Walters, M.E. Herndon, M.D. Henry, C.S. Stipp, CD151 Promotes α3β1 Integrin-Dependent Organization of Carcinoma Cell Junctions and Restrains Collective Cell Invasion, Cancer Biol. Ther. (2015) 0. https://doi.org/10.1080/15384047.2015.1095396.

[38] M. Shigeta, N. Sanzen, M. Ozawa, J. Gu, H. Hasegawa, K. Sekiguchi, CD151 regulates epithelial cell–cell adhesion through PKC- and Cdc42-dependent actin cytoskeletal reorganization, J Cell Biol. 163 (2003) 165–176. https://doi.org/10.1083/jcb.200301075.

[39] Q. Li, X.H. Yang, F. Xu, C. Sharma, H.-X. Wang, K. Knoblich, I. Rabinovitz, S.R. Granter, M.E. Hemler, Tetraspanin CD151 plays a key role in skin squamous cell carcinoma, Oncogene. 32 (2013) 1772–1783. https://doi.org/10.1038/onc.2012.205.

[40] N. Sachs, P. Secades, L. van Hulst, J.-Y. Song, A. Sonnenberg, Reduced susceptibility to two-stage skin carcinogenesis in mice with epidermis-specific deletion of CD151, J. Invest. Dermatol. 134 (2014) 221–228. https://doi.org/10.1038/jid.2013.280.

[41] Sterk LMT, Geuijen CAW, van den Berg JG, Claessen N, Weening JJ, Sonnenberg A. Association of the tetraspanin CD151 with the laminin-binding integrins alpha3beta1, alpha6beta1, alpha6beta4 and alpha7beta1 in cells in culture and in vivo. J. Cell. Sci. 2002;115(Pt 6):1161–73[42] Yauch RL, Berditchevski F, Harler MB, Reichner J, Hemler ME. Highly stoichiometric, stable, and specific association of integrin alpha3beta1 with CD151 provides a major link to phosphatidylinositol 4-kinase, and may regulate cell migration. Mol. Biol. Cell. 1998;9(10):2751–65[43] Scales TME, Jayo A, Obara B, Holt MR, Hotchin NA, Berditchevski F, et al. α3β1 integrins regulate CD151 complex assembly and membrane dynamics in carcinoma cells within 3D environments. Oncogene. 2013;32(34):3965–79[44] Palmer TD, Martínez CH, Vasquez C, Hebron KE, Jones-Paris C, Arnold SA, et al. Integrin-free tetraspanin CD151 can inhibit tumor cell motility upon clustering and is a clinical indicator of prostate cancer progression. Cancer Res. 2014;74(1):173–87

[45] Y. Saeki, T. Nagashima, S. Kimura, M. Okada-Hatakeyama, An ErbB receptor-mediated AP-1 regulatory network is modulated by STAT3 and c-MYC during calcium-dependent keratinocyte differentiation, Exp. Dermatol. 21 (2012) 293–298. https://doi.org/10.1111/j.1600-0625.2012.01453.x.

[46] X.-D. Peng, P.-Z. Xu, M.-L. Chen, A. Hahn-Windgassen, J. Skeen, J. Jacobs, D. Sundararajan, W.S. Chen, S.E. Crawford, K.G. Coleman, N. Hay, Dwarfism, impaired skin development, skeletal muscle atrophy, delayed bone development, and impeded adipogenesis in mice lacking Akt1 and Akt2, Genes Dev. 17 (2003) 1352–1365. https://doi.org/10.1101/gad.1089403.

[47] Ramovs V, Krotenberg Garcia A, Song JY, de Rink I, Kreft M, Goldschmeding R, Sonnenberg A. Integrin α3β1 in hair bulge stem cells modulates CCN2 expression and promotes skin tumorigenesis. Life Sci Alliance. 2020; 3(7):e202000645.

[48] T.M. Kinsella, G.P. Nolan, Episomal Vectors Rapidly and Stably Produce High-Titer Recombinant Retrovirus, Human Gene Therapy. 7 (1996) 1405–1413. https://doi.org/10.1089/hum.1996.7.12-1405.

[49] J.F. Bromberg, M.H. Wrzeszczynska, G. Devgan, Y. Zhao, R.G. Pestell, C. Albanese, J.E. Darnell, Stat3 as an oncogene, Cell. 98 (1999) 295–303.

[50] S. Huang, M. Hölzel, T. Knijnenburg, A. Schlicker, P. Roepman, U. McDermott, M. Garnett, W. Grernrum, C. Sun, A. Prahallad, F.H. Groenendijk, L. Mittempergher, W. Nijkamp, J. Neefjes, R. Salazar, P. Ten Dijke, H. Uramoto, F. Tanaka, R.L. Beijersbergen, L.F.A. Wessels, R. Bernards, MED12 controls the response to multiple cancer drugs through regulation of TGF-β receptor signaling, Cell. 151 (2012) 937–950. https://doi.org/10.1016/j.cell.2012.10.035.

[51] T. Shibue, R.A. Weinberg, Integrin beta1-focal adhesion kinase signaling directs the proliferation of metastatic cancer cells disseminated in the lungs, Proc. Natl. Acad. Sci. U.S.A. 106 (2009) 10290–10295. https://doi.org/10.1073/pnas.0904227106.

[52] L. Cong, F.A. Ran, D. Cox, S. Lin, R. Barretto, N. Habib, P.D. Hsu, X. Wu, W. Jiang, L.A. Marraffini, F. Zhang, Multiplex genome engineering using CRISPR/Cas systems, Science. 339 (2013) 819–823. https://doi.org/10.1126/science.1231143.

[53] C.T. Rueden, J. Schindelin, M.C. Hiner, B.E. DeZonia, A.E. Walter, E.T. Arena, K.W. Eliceiri, ImageJ2: ImageJ for the next generation of scientific image data, BMC Bioinformatics. 18 (2017) 529. https://doi.org/10.1186/s12859-017-1934-z.

[54] J. Schindelin, I. Arganda-Carreras, E. Frise, V. Kaynig, M. Longair, T. Pietzsch, S. Preibisch, C. Rueden, S. Saalfeld, B. Schmid, J.-Y. Tinevez, D.J. White, V. Hartenstein, K. Eliceiri, P. Tomancak, A. Cardona, Fiji: an open-source platform for biological-image analysis, Nature Methods. 9 (2012) 676–682. https://doi.org/10.1038/nmeth.2019.

[55] Y. Fradet, C. Cordon-Cardo, T. Thomson, M.E. Daly, W.F. Whitmore, K.O. Lloyd, M.R. Melamed, L.J. Old, Cell surface antigens of human bladder cancer defined by mouse monoclonal antibodies, Proc. Natl. Acad. Sci. U.S.A. 81 (1984) 224–228.

[56] D. Ivanyi, A. Ansink, E. Groeneveld, P.C. Hageman, W.J. Mooi, A.P.M. Heintz, New monoclonal antibodies recognizing epidermal differentiation-associated keratins in formalin-fixed, paraffin-embedded tissue. Keratin 10 expression in carcinoma of the vulva, The Journal of Pathology. 159 (1989) 7–12. https://doi.org/10.1002/path.1711590105.

[57] N. Sachs, M. Kreft, M.A. van den Bergh Weerman, A.J. Beynon, T.A. Peters, J.J. Weening, A. Sonnenberg, Kidney failure in mice lacking the tetraspanin CD151, J. Cell Biol. 175 (2006) 33–39. https://doi.org/10.1083/jcb.200603073.

[58] K.B. Jensen, R.R. Driskell, F.M. Watt, Assaying proliferation and differentiation capacity of stem cells using disaggregated adult mouse epidermis, Nat Protoc. 5 (2010) 898–911. https://doi.org/10.1038/nprot.2010.39.

[59] G.O. Delwel, A.A. de Melker, F. Hogervorst, L.H. Jaspars, D.L. Fles, I. Kuikman, A. Lindblom, M. Paulsson, R. Timpl, A. Sonnenberg, Distinct and overlapping ligand specificities of the alpha 3A beta 1 and alpha 6A beta 1 integrins: recognition of laminin isoforms, Mol. Biol. Cell. 5 (1994) 203–215.

SUPPLEMENTARY FIGURES

Supplementary figure 1

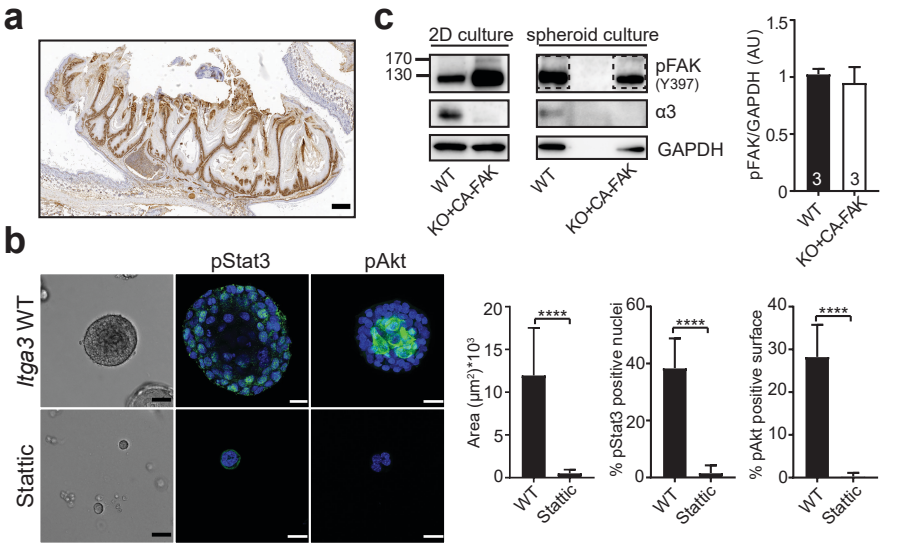

(**a**) IHC staining for integrin α3β1 in papilloma, formed after long-term DMBA/TPA-treatment of *Itgα3*-WT mice (Scale: 500 µm). (**b**) Representative bright field/IF images and quantifications of the area (n=80), pStat3 (Y705)-positive nuclei (n=20) and pAkt (S473)-positive area (n=20) of non-treated and 2 µM stattic-treated *Itgα3*-WT spheroids. Scale: 20 µm (IF), 50 µm (bright field). Statistics: mean ± SD, unpaired t test, ****P<0.0001. (**c**) Left: WB showing pFAK (Y397) expression in *Itgα3*-WT and *Itgα3*-KO MSCC keratinocytes transfected with a construct encoding constitutively active FAK (CA-FAK), grown in 2D or as spheroids. Even though CA-FAK construct is only expressed at low levels in spheroids (upper band), this suffices for the downstream activation of Akt and Stat3, as well as for activation of endogenous FAK (lower band). Right: quantification of total pFAK expression in spheroids (as indicated by the dash-line box) Statistics: mean ± SD

Supplementary figure 2

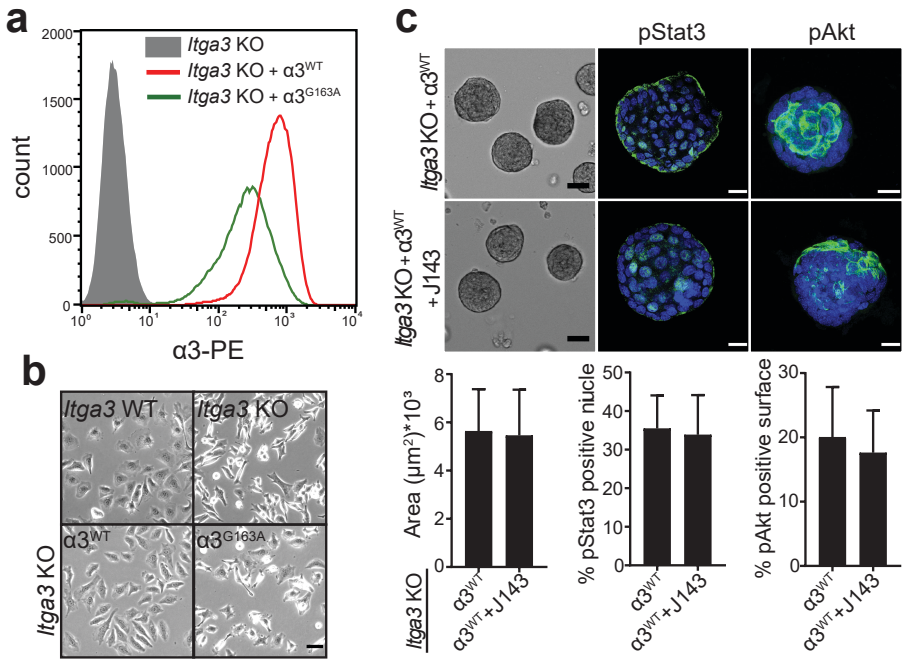

(**a**) Histogram of surface levels of α3β1 in MSCC *Itga3*-KO spheroids and MSCC *Itga3*-KO spheroids with stable expression of $\alpha3^{WT}$ or α3 laminin-binding mutant G163A ($\alpha3^{G163A}$). (**b**) MSCC *Itga3*-KO and MSCC-$\alpha3^{G163A}$ show reduced adhesion to laminin-rich matrix compared to MSCC *Itga3*-WT and MSCC-$\alpha3^{WT}$ keratinocytes. (**c**) Representative bright field/IF images and quantifications of the area (n=80), pStat3 (Y705)-positive nuclei (n=20) and pAkt (S473)-positive area (n=28) of *Itga3*KO spheroids rescued with human $\alpha3^{WT}$ construct and treated with function-blocking J143 antibody (1µg/ml) (Scale: 20µm (IF), 50µm (bright field)). Statistics: mean ± SD, unpaired t test.

Supplementary figure 3

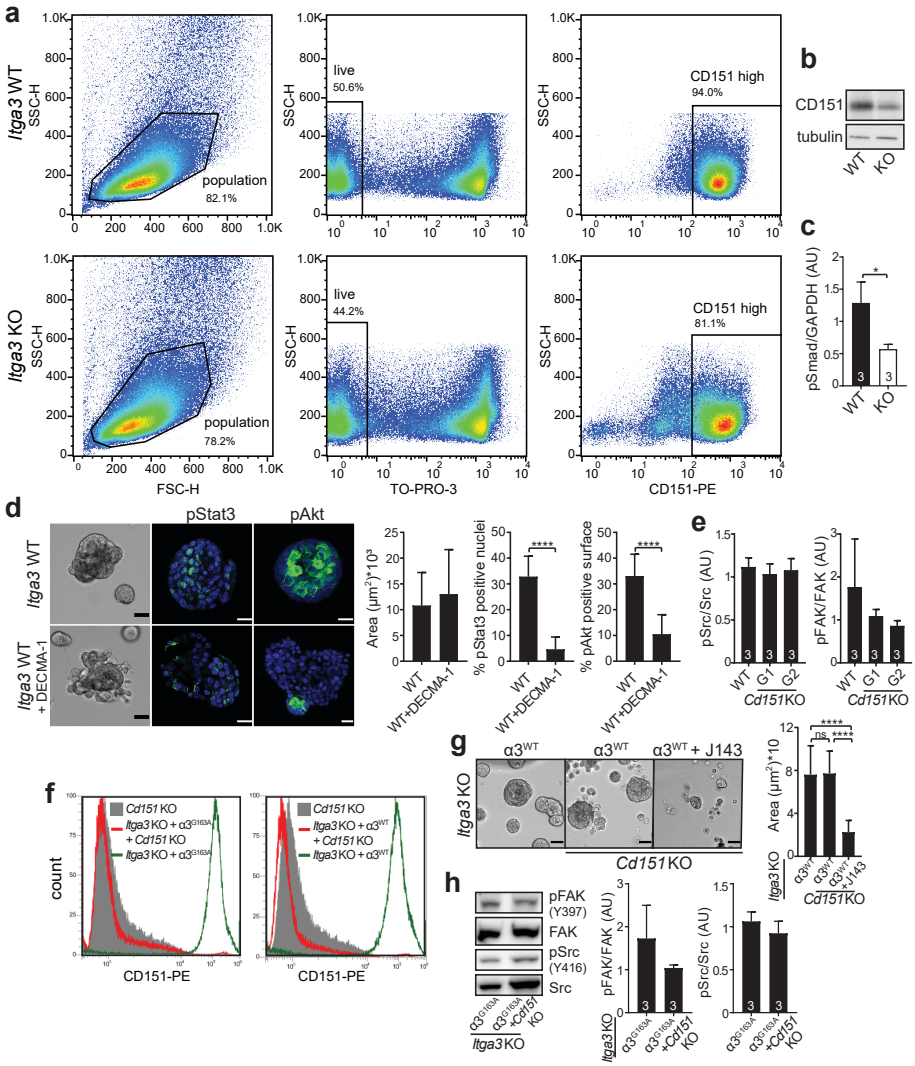

(**a**) Representative gating strategy of flow cytometry quantifications from Fig. 4a. (**b**) WB showing reduced expression of CD151 upon the deletion of α3β1 in mouse epidermis. (**c**) Quantification of the WB from the figure 4d. (**d**) Representative bright field/IF images and quantifications of the area (n=80), pStat3 (Y705)-positive nuclei (n=20) and pAkt (S473)-positive area (n=25) of *Itga3*-WT spheroids treated with function-blocking DECMA-1 antibody (10 µg ml−1) (Scale: 20 µm (IF), 50 µm (bright field)). (**e**) Quantification of the WB from the figure 4e. (**f**) Histogram of surface levels of CD151 in MSCC-*Cd151* KO, -α3^{G163A}, -α3^{WT} spheroids and MSCC-α3^{G163A} and -α3^{WT} spheroids with CD151 deletion. (g) Bright-field images and quantifications (n=85) of the size of MSCC-α3^{WT} spheroids, -α3^{WT} *Cd151* KO and -α3^{WT} *Cd151* KO spheroids treated with α3-blocking J143 antibody (10 µg ml−1). Scale: 50 µm. (h) WB and quantification of the pFAK and pSrc levels in MSCC-α3^{G163A} and MSCC-α3^{G163A} spheroids with deletion of *Cd151*. Statistics: mean ± SD, c-d, h: unpaired t test, e, g: Sidak's multiple comparisons test, *P<0.05, ****P<0.0001.

Supplementary figure 4

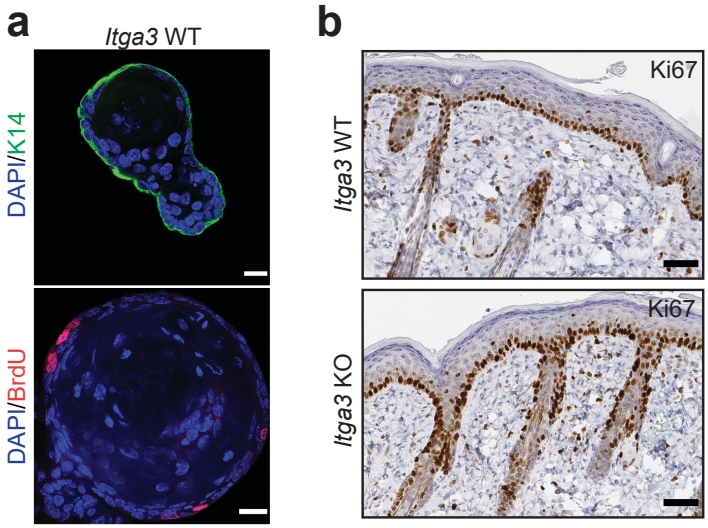

(**a**) IF staining of *Itga3*-WT MSCC spheroids showing keratin-14 expression and BrdU-positive proliferating keratinocytes in outer cell layer. (**b**) Ki67 staining of short-term DMBA/TPA-treated *Itga3*-WT and KO skin shows that majority of suprabasal keratinocytes are non-mitotic regardless of the presence of α3.